CHEMICALLY REACTING ON MHD BOUNDARY-LAYER FLOW OF NANOFLUIDS OVER A NON-LINEAR STRETCHING SHEET WITH HEAT SOURCE/SINK AND THERMAL RADIATION

by

Oluwole D. MAKINDE[a*], Fazle MABOOD[b], and Mohammed S. IBRAHIM[c],

[a] Faculty of Military Science, Stellenbosch University, Saldanha, South Africa
[b] Department of Mathematics, University of Peshawar, Peshawar, Pakistan
[c] Department of Mathematics, GITAM University, Visakhapatnam, Andhra Pradesh, India

Original scientific paper
https://doi.org/10.2298/TSCI151003284M

In this paper, steady 2-D MHD free convective boundary-layer flows of an electrically conducting nanofluid over a non-linear stretching sheet taking into account the chemical reaction and heat source/sink are investigated. The governing equations are transformed into a system of non-linear ODE using suitable similarity transformations. Analytical solution for the dimensionless velocity, temperature, concentration, skin friction coefficient, heat and mass transfer rates are obtained by using homotopy analysis method. The obtained results show that the flow field is substantially influenced by the presence of chemical reaction, radiation, and magnetic field.

Key words: *chemical reaction, homotopy analysis method, thermal radiation, MHD, nanofluids, stretching sheet*

Introduction

The concept of a nanofluid has been advanced by Choi [1] who showed substantial augmentation of heat transported in suspensions of copper or aluminum nanoparticles in water and other liquids. Nanofluids are a new kind of fluid. They are dispersions of nanoparticles in liquids that are permanently suspended by Brownian motion. By using different solvents and particles we hope to create composite fluids of widely variable and perhaps completely new properties. The heat transport properties of nanofluids depend on the thermal properties, concentration size and shape of suspended nanoparticles. A nanofluid is a more or less uniform dispersion of solid particles with small diameters measured in nanometers. A large number of experimental and theoretical studies have been carried out by numerous researchers on thermal conductivity of nanofluids [2, 3]. A comprehensive survey of convective transport in nanofluids has been employed by Buongiorno [4], who gave a satisfactory explanation for the abnormal increase of the thermal conductivity. Buongiorno and Hu [5], studied on the nanofluid coolant in advanced nuclear systems.

It is now well accepted fact that the terms MHD, thermal radiation and heat generation extensively appear in various engineering processes. The MHD is significant in the control of boundary-layer flow and metallurgical processes. Again the thermal radiation and heat generation possessions may arise in high temperature ingredients processing operations. Ingredients

* Corresponding author, e-mail: makinded@gmail.com

may be intelligently designed therefore with judicious implementation of radiative heating to produce the desired characteristics. This recurrently occurs in agriculture, engineering, plasma studies, and petroleum industries. Numerous flow complications under different aspects have been considered by the several scholars.

Vajravelu and Hadjinicalaou [6] scrutinized the heat transfer characteristics over a stretching surface with viscous dissipation in the presence of internal heat generation or absorption. The effect of radiation on convective heat transfer problems have been examined by a number of researchers using principally algebraic approximations for the radiative transfer simulation. Takhar *et al*. [7] employed a differential non-gray gas approximation to study non-linear gas dynamics in a permeable material. Seddeek [8] evaluated the effects of radiation and variable viscosity on hydromagnetic convection flow with an aligned magnetic field using a numerical method and a flux approximation for radiation. Free convection flow of a nanofluid over a linearly stretching sheet in presence of magnetic field has been studied by Hamad [9]. Habibi *et al*. [10] analyzed the MHD flow of nanofluid over a non-linear stretching sheet with effects of viscous dissipation and variable magnetic field. Very recently a number of studies of MHD boundary-layer fluid flow with the effects of thermal radiation and nanofluid were reported in the literature [11-17]. Heat and mass transfer problems with a chemical reaction have received a considerable amount of attention in recent years. In processes such as drying, evaporation, energy transfer in a cooling tower and the flow in a desert cooler, heat and mass transfer occur simultaneously. Anwar *et al*. [18] studied the conjugate effects of heat and mass transfer of nanofluids over a non-linear stretching sheet. Khan and Pop [19] studied boundary-layer heat-mass transfer free convection flows also in porous media of a nanofluid past a stretched sheet. Shakhaoath *et al*. [20] analyzed the boundary-layer nanofluid flow with MHD radiative possessions. Chamka [21] studied the MHD flow over a uniformly stretched vertical permeable surface subject to a chemical reaction. Afify [22] analyzed the MHD free convective flow and mass transfer over a stretching sheet with a homogeneous chemical reaction of order n (where n was taken to be 0, 1, 2 or 3). Chemical reaction effects on MHD heat and mass transfer flow of nanofluid near the stagnation point over a permeable stretching surface in presence of heat source was carried out by Gireesha and Rudraswamy [23]. Olanrewaju and Makinde [24] reported a numerical solution for the combined effects of thermal diffusion and thermo diffusion on chemically reacting MHD boundary-layer flow with heat and mass transfer past a moving permeable surface.

Homotopy analysis method (HAM), proposed by Liao [25], is a very powerful method and has been employed by numerous researchers in various physical phenomena [26, 27]. In this paper, we extend the results of the model presented by Poornima and Bhaskar [13] for chemical reaction and heat source/sink. We shall apply HAM to solve the similarity equations obtained from the governing boundary-layer equations with the help of similarity transformations.

Mathematical formulation

A steady 2-D boundary-layer flow of an incompressible electrically conducting and radiating nanofluid past a stretching surface is considered under the assumptions that the external pressure on the stretching sheet in the x-direction is having diluted nanoparticles. The x-axis is taken along the stretching surface and y-axis normal to it. A uniform stress leading to equal and opposite forces is applied along the x-axis so that the sheet is stretched, keeping the origin fixed. The stretching velocity is assumed to be $U_w(x) = U_0 x^m$ where U_0 the uniform velocity is and m ($m \geq 0$) is a constant parameter. The fluid

is considered to be a gray, absorbing emitting radiation but non-scattering medium. A uniform magnetic field is applied in the transverse direction to the flow. The fluid is assumed to be slightly conducting, so that the magnetic Reynolds number is much less than unity and hence the induced magnetic field is negligible in comparison with the applied magnetic field. Also, there is chemical reaction between the diffusing species and the fluid. Employing the Oberbeck-Boussinesq approximation, the governing equations of the flow field can be written in the dimensional form as [10-13]:

$$\frac{\partial u}{\partial x}+\frac{\partial v}{\partial y}=0 \tag{1}$$

$$\rho_f\left(u\frac{\partial u}{\partial x}+v\frac{\partial u}{\partial y}\right)=-\frac{\partial p}{\partial x}+\mu\frac{\partial^2 u}{\partial y^2}+(1-C_\infty)\rho_{f_\infty}\beta_T g(T-T_\infty)-(\rho_p-\rho_{f_\infty})\beta_C g(C-C_\infty)-\sigma B_0^2 u \tag{2}$$

$$u\frac{\partial T}{\partial x}+v\frac{\partial T}{\partial y}=\alpha\frac{\partial^2 T}{\partial y^2}-\frac{1}{(\rho c)_f}\frac{\partial q_r}{\partial y}+\frac{Q'}{(\rho c)_f}(T-T_\infty)+\tau\left[D_B\left(\frac{\partial T}{\partial y}\frac{\partial C}{\partial y}\right)+\frac{D_T}{T_\infty}\left(\frac{\partial T}{\partial y}\right)^2\right] \tag{3}$$

$$u\frac{\partial C}{\partial x}+v\frac{\partial C}{\partial y}=D_B\frac{\partial^2 C}{\partial y^2}+\frac{D_T}{T_\infty}\frac{\partial^2 T}{\partial y^2}-K_1 C \tag{4}$$

where u and v are the velocity components in the x- and y-directions, respectively, g – the acceleration due to gravity, μ – the viscosity, ρ_f – the density of the base fluid, ρ_p – the density of the nanoparticle, β_T – the coefficient of volumetric thermal expansion, β_c – the coefficient of volumetric concentration expansion, T – the temperature of the nanofluid, C – the concentration of the nanofluid, T_w – the temperature along the stretching sheet, C_w – the concentration along the stretching sheet, T_∞ – the ambient temperature of the nanofluid, C_∞ – the ambient concentration of the nanofluid, D_B – the Brownian diffusion coefficient, D_T – the thermophoresis coefficient, B_0 – the magnetic induction, q_r – the radiative heat flux, $(\rho c)_p$ – the heat capacitance of the nanoparticles, $(\rho c)_f$ – the heat capacitance of the nanofluid, $\alpha = k/(\rho c)_f$ – the thermal diffusivity parameter, k – the thermal conductivity, $\tau = (\rho c)_p/(\rho c)_f$ – the ratio between the effective heat capacity of the nanoparticles material and heat capacity of the nanofluid, Q' – the coefficient of heat generation parameter, and k_1 – the rate of chemical reaction parameter.

$$u=U_w(x)=U_0 x^m, \quad v=0, \quad T=T_w, \quad C=C_w, \quad \text{at} \quad y=0 \tag{5}$$

$$u\to 0, \quad v\to 0, \quad T\to T_\infty, \quad C\to C_\infty, \quad \text{at} \quad y\to\infty \tag{6}$$

By using the Rosseland approximation [14-17, 20], the radiative heat flux, q_r, is given by:

$$q_r=-\frac{4\sigma_s}{3k_e}\frac{\partial T^4}{\partial y}\cong-\frac{16\sigma_s T_\infty^3}{3k_e}\frac{\partial T}{\partial y} \tag{7}$$

where σ_s is the Stephen-Boltzmann constant and k_e – the mean absorption coefficient. It should be noted that by using the Rosseland approximation, the present analysis is limited to optically thick fluids. The temperature difference within the flow is assumed to be sufficiently small, then T^4 in eq. (7) can be easily linearized about T_∞ to give $T^4 \cong 4T_\infty^3 - 3T_\infty^4$. Invoking eqs. (7) and (3) gets modified:

$$u\frac{\partial T}{\partial x}+v\frac{\partial T}{\partial y}=\frac{k}{(\rho c)_f}\frac{\partial^2 T}{\partial y^2}+\frac{16\sigma_s T_\infty^3}{3k_e(\rho c)_f}\frac{\partial^2 T}{\partial y^2}+\frac{Q'}{(\rho c)_f}(T-T_\infty)+\tau\left[D_B\left(\frac{\partial T}{\partial y}\frac{\partial C}{\partial y}\right)+\frac{D_T}{T_\infty}\left(\frac{\partial T}{\partial y}\right)^2\right] \tag{8}$$

Using the steam function $\psi = \psi(x, y)$, the velocity components u and v are defined as $u = \partial\psi/\partial y$, $v = -\partial\psi/\partial x$. Assuming that the external pressure on the sheet, in the direction having diluted nanoparticles, to be constant, the similarity transformations is taken:

$$\psi = \sqrt{\frac{2\nu U_0 x^{m+1}}{m+1}} f(\eta),\ \ \theta(\eta) = \frac{T - T_\infty}{T_w - T_\infty},\ \ \phi(\eta) = \frac{C - C_\infty}{C_w - C_\infty},\ \ \eta = \sqrt{\frac{(m+1)U_0 x^{m-1}}{2\nu}},\ \ Nr = \frac{kk_e}{4\sigma_s T_\infty^3},\ \ R = \frac{4}{3Nr}$$

$$\delta = \frac{\mathrm{Gm}}{\mathrm{Re}_x^{3/2}},\ \ \mathrm{Pr} = \frac{\nu}{\alpha},\ \ \nu = \frac{\mu}{\rho_f},\ Nb = \frac{\tau D_B (C_w - C_\infty)}{\upsilon},\ Gr = \frac{(1 - C_\infty)\rho_{f_\infty} gn(T_w - T_\infty)}{\rho_f \nu^2 \mathrm{Re}_x^{1/2}},\ \lambda = \frac{\mathrm{Gr}}{\mathrm{Re}_x^{3/2}},\ \mathrm{Le} = \frac{\nu}{D_B} \quad (9)$$

$$\gamma = \frac{k_1 U_w (C_w - C_\infty)}{\nu},\ \ \mathrm{Re}_x = \frac{U_w(x)x}{\nu},\ \ Nt = \frac{\tau D_T (T_w - T_\infty)}{\nu T_\infty},\ \ Q' = \frac{QU_w(x)}{x\nu},\ \ \mathrm{Gr} = \frac{(\rho_p - \rho_{f_\infty})gn_1(C_w - C_\infty)}{\rho_f \nu^2 \mathrm{Re}_x^{1/2}}$$

In view of the similarity transformations, the eqs. (2)-(4) are reduce to:

$$f''' + ff'' - \frac{2m}{m+1}(f')^2 + \frac{2}{m+1}(\lambda\theta - \delta\phi) - Mf' = 0 \quad (10)$$

$$(1+R)\theta'' + \mathrm{Pr}\, f\theta' + \mathrm{Pr}\, Nb\theta'\phi + \mathrm{Pr}\, Nt(\theta')^2 + \mathrm{Pr}\, Q\theta = 0 \quad (11)$$

$$\phi'' + \mathrm{Le} f\phi' + \frac{Nt}{Nb}\theta'' - \gamma\phi = 0 \quad (12)$$

where λ is the buoyancy parameter, δ – the solute buoyancy parameter, Pr – the Prandtl number, Le – the Lewis number, ν – the kinematic viscosity of the nanofluid, Nb – the Brownian motion parameter, Nt – the thermophoresis parameter, Re_x – the local Reynolds number based on the stretching velocity, Gr – the local thermal Grashof number, Gm – the local concentration Grashof number, R – the radiation parameter, Q – the heat generation parameter, γ – the chemical reaction parameter, and f, θ, ϕ – the dimensionless stream functions, temperature, concentration, respectively. Here, β_T and β_C are proportional to x^{-3}, that is $\beta_T = nx^{-3}$ and $\beta_C = n_1 x^{-3}$ where n and n_1 are the constants of proportionality. The corresponding boundary conditions are:

$$f(0) = 0,\quad f'(0) = 1,\quad \theta(0) = 1,\quad \phi(0) = 1,\quad f'(\infty) = 0,\quad \theta(\infty) = 0,\quad \phi(\infty) = 0 \quad (13)$$

The skin friction coefficient, C_f, Nusselt number, and Sherwood number are important physical parameters given by:

$$C_f = \frac{1}{\sqrt{2(m+1)}}\mathrm{Re}_x^{1/2} f''(0),\ \ \mathrm{Nu} = -\sqrt{\frac{2}{m+1}}\mathrm{Re}_x^{-1/2}\theta'(0),\ \ \mathrm{Sh} = -\sqrt{\frac{2}{m+1}}\mathrm{Re}_x^{-1/2}\phi'(0) \quad (14)$$

Homotopy analysis solution

In order to solve eqs. (10)-(13) analytically using HAM, we express the solutions by the set of base functions as $\{\eta^k \exp(-n\eta)$: $k \geq 0$, $n \geq 0$ are integers$\}$ in the form:

$$\begin{cases} f(\eta) = \sum_{n=0}^{\infty}\sum_{k=0}^{\infty} a_{m,n}^k \eta^k \exp(-n\eta) \\ \theta(\eta) = \sum_{n=0}^{\infty}\sum_{k=0}^{\infty} b_{m,n}^k \eta^k \exp(-n\eta) \\ \phi(\eta) = \sum_{n=0}^{\infty}\sum_{k=0}^{\infty} c_{m,n}^k \eta^k \exp(-n\eta) \end{cases} \quad (15)$$

where $a^k_{m,n}$, $b^k_{m,n}$, $c^k_{m,n}$ are the coefficients. Then from eqs. (10)-(13), it is a straightforward matter to choose, $f_0(\eta) = 1 - e^{-\eta}$, $\theta_0(\eta) = e^{-\eta}$, $\phi_0(\eta) = 1 - e^{-\eta}$, as our initial approximations for $f(\eta)$, $\theta(\eta)$, and $\varphi(\eta)$, respectively. The auxiliary linear operators are then chosen:

$$L(f) = \frac{\mathrm{d}^3 f}{\mathrm{d}\eta^3} - \frac{\mathrm{d}f}{\mathrm{d}\eta}, \quad L(\theta) = \frac{\mathrm{d}^2\theta}{\mathrm{d}\eta^2} - \theta, \quad L(\phi)\frac{\mathrm{d}^2\phi}{\mathrm{d}\eta^2} - \phi \tag{16}$$

with the following properties:

$$L_f\left(C_1 + C_2 e^{\eta} + C_3 e^{-\eta}\right) = 0,\ L_\theta\left(C_4 e^{\eta} + C_5 e^{-\eta}\right) = 0,\ L_\phi\left(C_6 e^{\eta} + C_7 e^{-\eta}\right) = 0 \tag{17}$$

where C_i (i = 1-7) are arbitrary constants. Let $q \in [0,1]$ represent an embedding parameter and $\hbar_f$, $\hbar_\theta$, and $\hbar_\phi$ denote the non-zero auxiliary linear operators and construct the following zeroth order deformation equations:

$$(1-q)L_f\left[\hat{f}(\eta;q) - f_0(\eta)\right] = q\hbar_f N_{\mathrm{f}}\left[\hat{f}(\eta;q)\right] \tag{18}$$

$$(1-q)L_\theta\left[\hat{\theta}(\eta;q) - \theta_0(\eta)\right] = q_\theta\hbar_\theta N_\theta\left[\hat{\theta}(\eta;q), \hat{f}(\eta;q)\right] \tag{19}$$

$$(1-q)L_\phi\left[\hat{\phi}(\eta;q) - \phi_0(\eta)\right] = q\hbar_\phi N_\phi\left[\hat{\theta}(\eta;q), \hat{f}(\eta;q)\right], \tag{20}$$

subject to the boundary conditions:

$$\hat{f}(0;q) = 0, \quad \hat{f}'(0;q) = 1, \quad \hat{f}'(\infty;q) = 0, \quad \hat{\theta}(0;q) = 1, \quad \hat{\theta}(\infty;q) = 0$$
$$\hat{\phi}(0;q) = 1, \quad \hat{\phi}(\infty;q) = 0 \tag{21}$$

where the non-linear operators are defined:

$$N_f\left[\hat{f}(\eta;q)\right] = \begin{cases} \dfrac{\partial^3\hat{f}(\eta;q)}{\partial\eta^3} + \hat{f}(\eta;q)\dfrac{\partial^2\hat{f}(\eta;q)}{\partial\eta^2} - \dfrac{2m}{m+1}\left[\dfrac{\partial\hat{f}(\eta;q)}{\partial\eta}\right]^2 + \\ + \dfrac{2}{m+1}\left[\lambda\hat{\theta}(\eta;q) - \delta\hat{\phi}(\eta;q)\right] - M\left[\dfrac{\partial\hat{f}(\eta;q)}{\partial\eta}\right] \end{cases} \tag{22}$$

$$N_\theta\left[\hat{\theta}(\eta;q), \hat{f}(\eta;q)\right] = \begin{cases} (1+R)\dfrac{\partial^2\hat{\theta}(\eta;q)}{\partial\eta^2} + \mathrm{Pr}\,\hat{f}(\eta;q)\dfrac{\partial\hat{\theta}(\eta;q)}{\partial\eta} + \\ + \mathrm{Pr}\,Nb\dfrac{\partial\hat{\theta}(\eta;q)}{\partial\eta}\dfrac{\partial\hat{\phi}(\eta;q)}{\partial\eta} + \mathrm{Pr}\,Nt\left[\dfrac{\partial\hat{\theta}(\eta;q)}{\partial\eta}\right]^2 + \mathrm{Pr}\,Q\hat{\theta}(\eta;q) \end{cases} \tag{23}$$

$$N_\phi\left[\hat{\phi}(\eta;q), \hat{f}(\eta;q)\right] = \frac{\partial^2\hat{\phi}(\eta;q)}{\partial\eta^2} + \mathrm{Le}\hat{f}(\eta;q)\frac{\partial\hat{\phi}(\eta;q)}{\partial\eta} + \frac{Nt}{Nb}\frac{\partial^2\hat{\theta}(\eta;q)}{\partial\eta^2} - \gamma\left[\hat{\phi}(\eta;q)\right] \tag{24}$$

setting q = 0 and q = 1, we obtain from eqs. (18)-(21):

$$\hat{f}(\eta;0) = f_0(\eta),\ \hat{f}(\eta;1) = f(\eta),\ \hat{\theta}(\eta;0) = \theta_0(\eta),\ \hat{\theta}(\eta;1) = \theta(\eta),\ \hat{\phi}(\eta;0) = \phi_0(\eta),\ \hat{\phi}(\eta;1) = \phi(\eta) \tag{25}$$

Now let:

$$f_m(\eta) = \frac{1}{m!}\frac{\partial^m f(\eta;q)}{\partial q^m}\bigg|_{q=0}, \quad \theta_m(\eta) = \frac{1}{m!}\frac{\partial^m\theta(\eta;q)}{\partial q^m}\bigg|_{q=0}, \quad \phi_m(\eta) = \frac{1}{m!}\frac{\partial^m\phi(\eta;q)}{\partial q^m}\bigg|_{q=0} \tag{26}$$

and expanding $\hat{f}(q;\eta)$, $\hat{\theta}(q;\eta)$, $\hat{\phi}(q;\eta)$, by means of Taylor's theorem with respect to q, we obtain:

$$\hat{f}(q;\eta)=f_0(\eta)+\sum_{m=1}^{+\infty}f_m(\eta)q^m,\quad \hat{\theta}(q;\eta)=\theta_0(\eta)+\sum_{m=1}^{+\infty}\theta_m(\eta)q^m,\quad \hat{\phi}(q;\eta)=\phi_0(\eta)+\sum_{m=1}^{+\infty}\phi_m(\eta)q^m \tag{27}$$

The auxiliary parameters are properly chosen so that series (27) converge at $q = 1$ and thus:

$$f(\eta)=f(\eta)+\sum^{+\infty}f(\eta),\qquad \theta(\eta)=\theta_0(\eta)+\sum_{m=1}^{+\infty}\theta_m(\eta),\qquad \phi(\eta)=\phi_0(\eta)+\sum_{m=1}^{+\infty}\phi_m(\eta) \tag{28}$$

The resulting problems at the m^{th} order deformation are:

$$\begin{aligned}L_f\left[f_m(\eta)-\chi_m f_{m-1}(\eta)\right]&=\hbar_f \mathrm{R}_m^f(\eta)\\ L_\theta\left[\theta_m(\eta)-\chi_m\theta_{m-1}(\eta)\right]&=\hbar_\theta \mathrm{R}_m^\theta(\eta)\\ L_\phi\left[\phi_m(\eta)-\chi_m\phi_{m-1}(\eta)\right]&=\hbar_\phi \mathrm{R}_m^\phi(\eta)\end{aligned} \tag{29}$$

with

$$\mathrm{R}_m^f(\eta)=\begin{cases}f'''_{m-1}(\eta)+\sum_{k=0}^{m-1}f_k f''_{m-1-k}-\dfrac{2m}{m+1}\sum_{k=0}^{m-1}f'_k f'_{m-1-k}+\\ +\dfrac{2}{m+1}\left(\lambda\theta_{m-1-k}-\delta\phi_{m-1-k}\right)-Mf'_{m-1}(\eta)\end{cases}$$

$$\mathrm{R}_m^\theta(\eta)=\begin{cases}(1+R)\theta''_{m-1}(\eta)+\mathrm{Pr}\sum_{k=0}^{m-1}f_k\theta'_{m-1-k}+\mathrm{Pr}\,Nb\sum_{k=0}^{m-1}\theta'_k\phi'_{m-1-k}+\\ +\mathrm{Pr}\,Nt\sum_{k=0}^{m-1}\theta'_k\theta'_{m-1-k}+\mathrm{Pr}\,Q\theta_{m-1}(\eta)\end{cases} \tag{30}$$

$$\mathrm{R}_m^\phi(\eta)=\phi''_{m-1}(\eta)+\mathrm{Le}\sum_{k=0}^{m-1}f_k\phi'_{m-1-k}+\frac{Nt}{Nb}\theta''_{m-1}(\eta)-\gamma\phi_{m-1}(\eta),\ \chi_m=\begin{cases}0, & m\le 1\\ 1, & m>1\end{cases} \tag{31}$$

subject to boundary conditions:

$$f_m(0)=0,\ f'_m(0)=0,\ f'_m(\infty)=0,\ \theta_m(0)=0,\ \theta_m(\infty)=0,\ \phi_m(0)=0,\ \phi_m(\infty)=0 \tag{32}$$

The general solutions of eqs. (32)-(35) are expressed:

$$\begin{aligned}f_m(\eta)&=f_m^*(\eta)+C_1+C_2\exp(\eta)+C_3\exp(-\eta)\\ \theta_m(\eta)&=\theta_m^*(\eta)+C_4\exp(\eta)+C_5\exp(-\eta)\\ \phi_m(\eta)&=\phi_m^*(\eta)+C_6\exp(\eta)+C_7\exp(-\eta)\end{aligned} \tag{33}$$

where $f^*_m(\eta)$, $\theta^*_m(\eta)$, and $\phi^*_m(\eta)$ are the particular solutions and the constants are to be determined by the boundary condition at eq. (32).

Convergence of the HAM

The convergence of the series solution given by HAM depends strongly auxiliary parameters $\hbar_f$, $\hbar_\theta$, and $\hbar_\phi$. In order to choose appropriate values for these auxiliary parameters, the $\hbar_f$, $\hbar_\theta$, and $\hbar_\phi$ curves are displayed at 20th order approximations as shown in fig. 1. It is clear from fig. 1 that the solution for velocity field converges for $-1.45 \le \hbar_f \le -0.3$, the solution for the temperature profile converges for $-1.3 \le \hbar_\theta \le -0.3$, and the concentration distribution converge when $-1.1 \le \hbar_\phi \le -0.3$.

Results and discussion

Computations were carried out with HAM for several non-dimensional parameters. Convergence of the series solution up to 50th order of approximation is presented in tab. 1. It is clearly seen that the convergence is obtained after 25th order of approximation.

In order to validate the accuracy of the HAM technique, we have compared our HAM computation results of reduced Nusselt and Sherwood numbers with those available in open literature in tab. 2, which are in good agreement. The influence of the magnetic parameter on the velocity is shown in fig. 2(a). As the magnetic parameter increases, the velocity decreases. This is because, an application of the magnetic field within the boundary-layer produces a resistive type force known as Lorentz force which opposes the flow, and decelerate the fluid motion. The effect of the stretching parameter on the velocity is shown in fig. 2(b). It is found that, the velocity decreases as the stretching parameter increases.

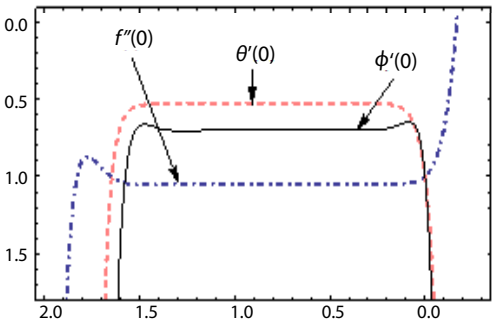

Figure 1. The $\hbar$-curves for the 20th order of approximation

Table 1. Convergence of HAM solutions for different order of approximations when Pr = 1.6, Le = 2, m = 1, $\lambda = \delta = \gamma = M = Nb = Nt = R = Q$ = 0.1, and $\hbar_f = \hbar_\theta = \hbar_\phi$ = –0.5

Order of approximation	$f'(0)$	$-\phi'(0)$	$-\theta'(0)$
1	–1.0250	0.76500	0.69167
5	–1.0482	0.54770	0.65699
15	–1.0482	0.52810	0.70309
25	–1.0482	0.52833	0.70321
50	–1.0482	0.52833	0.70321

Table 2. Comparison of reduced Nusselt and Sherwood numbers when Pr = Le = 10, $\lambda = \delta = \gamma = R = Q$ = 0, Pr = Le = 10

Parameters		Khan and Pop [19]		Anwar *et al.* [18]		Poornima and Reddy [13]		Present results	
Nb	Nt	$-\theta'(0)$	$-\phi'(0)$	$-\theta'(0)$	$-\phi'(0)$	$-\theta'(0)$	$-\phi'(0)$	$-\theta'(0)$	$-\phi'(0)$
0.1	0.1	0.9524	2.1294	0.9524	2.1294	0.952376	2.12939	0.952376	2.129388
0.2	0.2	0.3654	2.5152	0.3654	2.5152	0.365357	2.51522	0.365358	2.515217
0.3	0.3	0.1355	2.6088	0.1355	2.6088	0.135514	2.60881	0.135514	2.608812
0.4	0.4	0.0495	2.6038	0.0495	2.6038	0.049465	2.60384	0.049464	2.603839
0.5	0.5	0.0179	2.5731	0.0179	2.5731	0.017922	2.5731	0.017922	2.573099

Figure 3(a) shows the effect of the thermal buoyancy parameter on the velocity. Here, the positive buoyancy force acts like a favorable pressure gradient and hence accelerates the fluid in the boundary-layer. This results in higher velocity as thermal buoyancy parameter, λ, increases. The solute buoyancy parameter effect on the velocity is illustrated in fig. 3(b). It is noticed that as the solute buoyancy parameter increases, the velocity decreases. Figure 4(a) shows the effect of the radiation parameter on the dimensionless

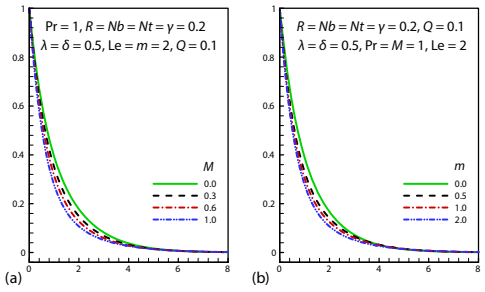

Figure 2. Effects of M and m on $f'(\eta)$

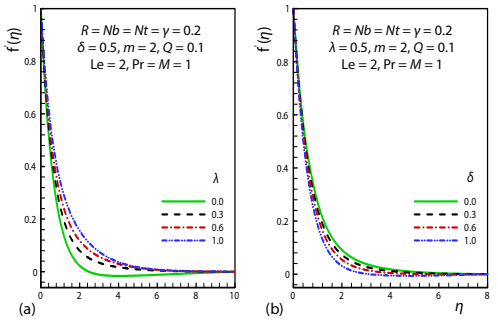

Figure 3. Effects of λ and δ on $f'(\eta)$

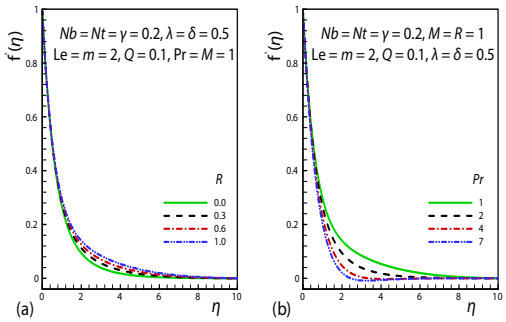

Figure 4. Effects of R and Pr on $f'(\eta)$

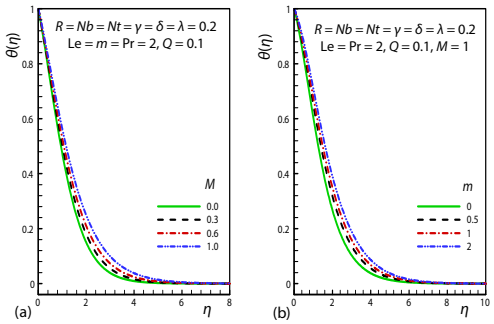

Figure 5. Effects of M and m on $\theta(\eta)$

Table 3. Values of C_f, Nu and Sh for different values of parameters when Pr = Le = 10, m = 2 and $\lambda = \delta$ = 1, $Nb = Nt$ = 0.2

M	R	Q	γ	$f''(0)$	$-\theta'(0)$	$-\phi'(0)$
0	0	0	0	– 1.042279	0.365079	2.502555
0.5				– 1.253209	0.361523	2.423311
1				– 1.434499	0.358418	2.355568
2				– 1.743398	0.352958	2.241402
1	0.2			– 1.431581	0.413446	2.303049
	0.4			– 1.428145	0.454384	2.261974
	0.8			– 1.420564	0.506944	2.204722
	1			– 1.416649	0.523156	2.184950
	0.5	–0.5		– 1.478308	1.096005	1.776694
		–0.2		– 1.451132	0.745432	2.043642
		0		– 1.426310	0.470676	2.244941
		0.2		– 1.391330	0.136955	2.478538
		0.5		– 1.282866	– 0.69288	3.004728
		0.1	0.1	– 1.409642	0.312585	2.385089
			0.3	– 1.407889	0.310428	2.441311
			0.5	– 1.406205	0.308369	2.496057
			1	– 1.402273	0.303606	2.627032

velocity. It is observed that as the radiation parameter increases, the velocity increases. Figure 4(b) depicts the effect of the Prandtl number on the velocity. It is noticed that, an increase in the Prandtl number makes the fluid to be more viscous, which leads to decrease in the velocity. Figures 5(a) and 5(b) depict temperature profile for magnetic field parameter and stretching parameter. It is observed that in both the cases an increase in magnetic field parameter or stretching parameter leads to increase in fluid temperature. The values of skin friction, Nusselt and Sherwood numbers for different values of parameters as illustrated in figs. 14-16 are displayed in tab. 3. The skin friction increases with M and decreases with R, Q (>0) and γ. Increase in M, γ, and Q (>0) decrease the Nu while an increase R and (Q < 0) will enhance the Nu. The Sh increases with Q (>0), γ but decreases with M and R.

From the figs. 6(a) and (b), it is observed that the temperature along the surface decreases for the case of increasing buoyancy parameter but increases in the case of increase solute buoyancy parameter. The effect of the radiation parameter on the temperature is depicted in fig. 7(a). It is seen that as the radiation parameter increases, temperature increases. Figure 7(b) shows the effect of the Prandtl number on the temperature. It is noticed that as the

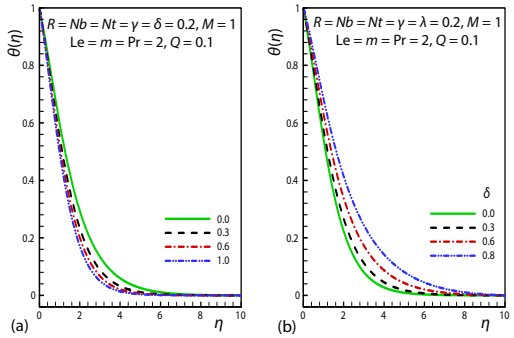

Figure 6. Effects of λ and δ on $\theta(\eta)$

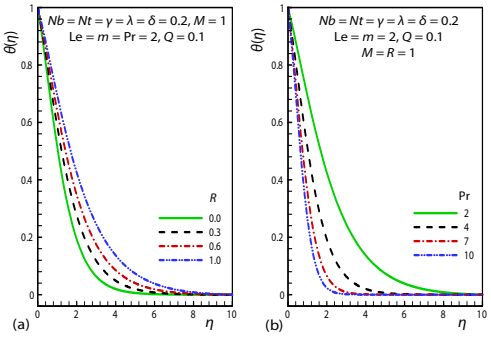

Figure 7. Effects of R and Pr on $\theta(\eta)$

Prandtl number increases, the temperature decreases. This is due to the fact that for smaller values of Prandtl number are equivalent to larger values of thermal conductivities and therefore heat is able to diffuse away from the stretching sheet.

The temperature profiles for various values of heat source parameter are shown in fig. 8(a). In fig. 8(a) it is identified that the temperature increases, as the heat source parameter increases. Figure 8(b) is graphical representation of temperature distributions for different values of the chemical reaction parameter. It is seen that the concentration of the fluid decreases with increase of chemical reaction parameter. The influence of the Brownian motion parameter and thermophoresis parameters are illustrated in figs. 9(a) and (b). It is clear that the temperature decreases, as the Brownian motion parameter increases, while temperature increases as the thermophoresis parameter increases.

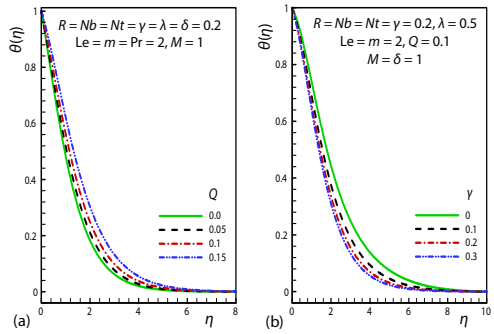

Figure 8. Effects of Q and γ on $\theta(\eta)$

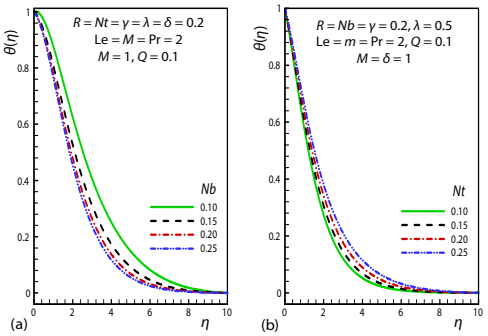

Figure 9. Effects of Nb and Nt on $\theta(\eta)$

The concentration profiles for different values of the magnetic field parameter and stretching parameter are shown in figs. 10(a) and (b), respectively. It is found that the concentration of the flow field increases as the magnetic field parameter or stretching parameter increases. The influences of the thermal and solute buoyancy parameters on the concentration field area shown in figs. 11(a) and (b), respectively. It is noticed that the concentration decreases as the thermal buoyancy parameter increases, but concentration increase with an increase of sol-

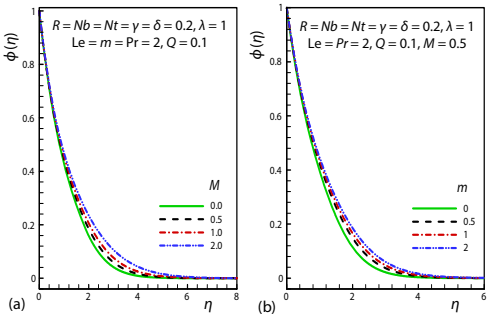

Figure 10. Effects of M and m on $\phi(\eta)$

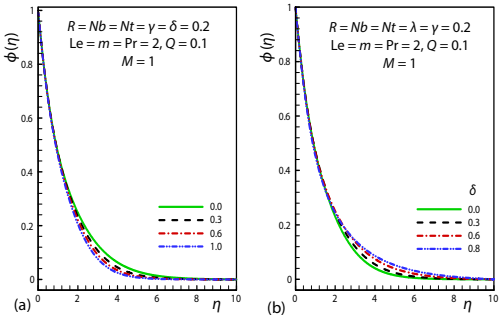

Figure 11. Effects of λ and δ on $\phi(\eta)$

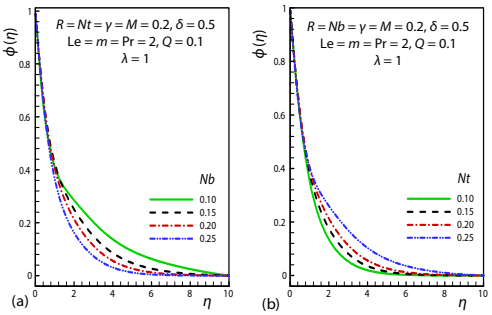

Figure 12. Effects of *Nb* and *Nt* on $\phi(\eta)$

ute buoyancy parameter. Figure 12(a) shows the effect of the Brownian motion parameter on the concentration profiles. It is observed that as Brownian motion parameter increases, the concentration decreases. The effect of the thermophoresis parameter on the concentration of the flow field is presented in fig. 12(b). We notice that the concentration increases as the thermophoresis parameter increases. The concentration profiles for different values of the chemical reaction parameter and Lewis number are shown in figs. 13(a) and (b), respectively. It is found that the concentration of the flow field decreases as the chemical reaction parameter and Lewis number increases.

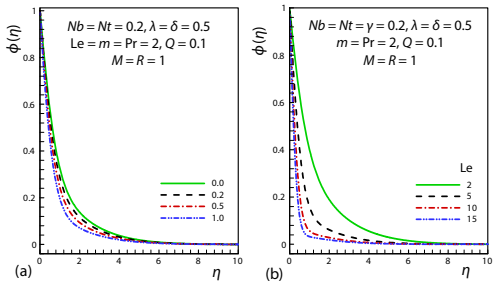

Figure 13. Effects of γ and Le on $\phi(\eta)$

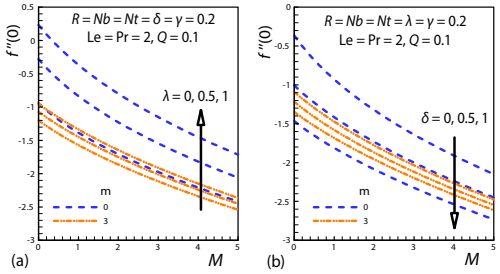

Figure 14. Effects of *M*, *m*, λ and δ on C_f

The effects of various physical parameters on skin friction coefficient, Nusselt number, and Sherwood number are shown in figs. 14-16. The skin friction coefficient increases with an increase magnetic field intensity but decreases with a combined increase in radiation parameter, heat source parameter, and chemical reaction. This may be attributed to an increase or decrease in the velocity gradient at the sheet surface as the parameter varies. The Nusselt number decreases with an increase in magnetic field, heat source and chemical reaction, while

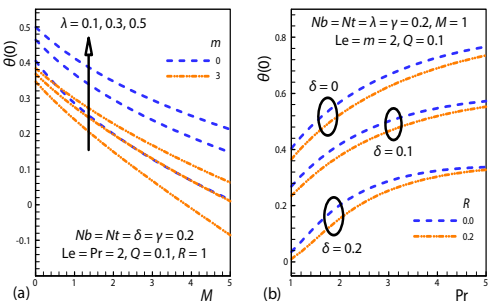

Figure 15. Effects of M, *m*, λ, δ, *R*, and Pr on Nu

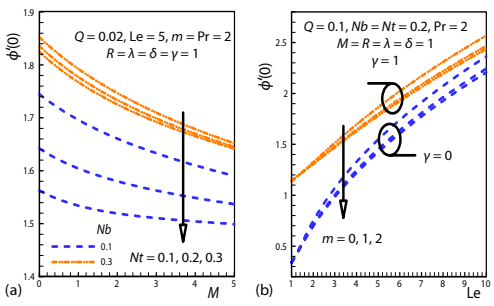

Figure 16. Effects of *M*, *Nb*, *Nt*, γ, *m*, and Le on Sh

an increase with heat sink and thermal radiation will enhance Nusselt number. It is interesting, to note that buoyancy parameter enhances both the heat and mass transfer rate at the sheet surface. Moreover, the Sherwood number increases with an increase in chemical reaction and heat source but decreases with an increase in magnetic field and thermal radiation.

Conclusions

In this paper, we have analyzed theoretically the effects of thermal radiation, chemical reaction on steady MHD heat and mass transfer flow of nanofluids over a non-linear stretching sheet with heat source. The transformed two-point non-linear boundary value problem has been solved with HAM. Good agreement of HAM solution is observed with those obtained by numerical methods. The present solutions have shown that the velocity decreases and temperature increases with magnetic field parameter. A rise in the radiation parameter raises the temperature as well as rate of heat transfer and the presence of radiation radiates the heat energy away from the fluid. It is the nanofluids property to enhance the thermal conductivity. There is a rise in the temperature with an increase in the heat generation, stretching parameters and solute buoyancy force and a fall with an increase in thermal buoyancy parameter and Prandtl number. Species concentration increases within the magnetic field, stretching parameter while the concentration decreases for an increase in the values of Lewis number, chemical reaction parameter, and Brownian motion parameter. Skin friction coefficient increases with an increase in the magnetic parameter and decreases with an increase in the radiation parameter. The increase in chemical reaction parameter decreases the dimensionless concentration in the concentration boundary-layer. Thus mass transfer rate increases with chemical reaction parameter.

References

[1] Choi, U. S., *Enhancing Thermal Conductivity of Fluids with Nanoparticles*, in: Developments and Applications of Non-Newtonian Flows, (Eds. D. A. Siginer, H. P. Wang), FED-Vol. 231/MD-66 ASME, New York, USA, 1995, pp. 99-105
[2] Fan, J., Wang, L., Heat Conduction in Nanofluids: Structure-Property Correlation, *Int. J. Heat Mass Transf.*, *54* (2011), 19-20, pp. 4349-4359
[3] Kleinstreuer, C., Feng, Y., Experimental and Theoretical Studies of Nanofluid Thermal Conductivity Enhancement: A Review, *Nanoscale Res Lett*, *6* (2011), 1, pp. 229-241
[4] Buongiorno, J., Convective Transport in Nanofluids, *J. Heat Transf.*, *128* (2005), 3, pp. 240-520
[5] Buongiorno, J., Hu, W., Nanofluid Coolants for Advanced Nuclear Power Plants, *Proceedings*, ICANPP Seoul, Korea, Curran Assoc Inc. 2005, pp. 15-19
[6] Vajravelu, K., Hadjinicalaou, A., Heat Transfer in a Viscous Fluid over a Stretching Sheet with Viscous Dissipation and Internal Heat Generation, *Int. Commun. Heat Mass Transf.*, *20* (1993), 3, pp. 417-430
[7] Takhar, H. S., *et al*., Computational Analysis of Coupled Radiation Convection Dissipative Flow in a Porous Medium Using the Keller-Box Implicit Difference Scheme, *Int. J. Energy Res*., *22* (1998), 2, pp. 141-159
[8] Seddeek, M. A., Effects of Radiation and Variable Viscosity on a MHD Free Convection Flow Past a Semi-Infinite Flat Plate with an Aligned Magnetic Field in the Case of Unsteady Flow, *Int. J. Heat Mass Transf.*, *45* (2002), 4, pp. 931-935
[9] Hamad, M. A. A., Analytical Solution of Natural Convection Flow of a Nanofluid over a Linearly Stretching Sheet in the Presence of Magnetic Field, *Int. Commun. Heat Mass Transf.*, *38* (2011), 4, pp. 487-492
[10] Habibi, M. M., *et al*., Mixed Convection MHD Flow of Nanofluid over a Nonlinear Stretching Sheet with Effects of Viscous Dissipation and Variable Magnetic Field, *Mechanika*, *18* (2012), Sept., pp. 415-423
[11] Sandeep, N., Sulochana, C., Dual Solutions of Radative MHD Nanofluid Flow over an Exponentially Stretching Sheet with Heat Generation/Absorptio,. *Appl. Nano Sci*., *6* (2015), 1, pp. 131-139
[12] Rana, P., Bhargava, R., Flow and Heat Transfer of a Nanofluid over a Non-Linearly Stretching Sheet: A Numerical Study, *Commun. Nonlinear Sci Numer. Simul*., *17* (2012), 1, pp. 212-226
[13] Poornima, T., Bhaskar, R. N., Radiation Effects on MHD Free Convective Boundary Layer Flow of Nanofluids over a Non-Linear Stretching Sheet, *Adv. Appl. Sci. Res*., *4* (2013), Jan., pp. 190-202

[14] Makinde, O. D., Free-Convection Flow with Thermal Radiation and Mass Transfer Past a Moving Vertical Porous Plate, *International Communications in Heat and Mass Transfer*, *32* (2005), 10, pp. 1411-1419
[15] Makinde, O. D., Ogulu, A., The Effect of Thermal Radiation on the Heat and Mass Transfer Flow of a Variable Viscosity Fluid Past a Vertical Porous Plate Permeated by a Transverse Magnetic Field, *Chemical Engineering Communications*, *195* (2008), 12, pp. 1575-1584
[16] Makinde, O. D., Moitsheki, R. J., On Non-Perturbative Techniques for Thermal Radiation Effect on Natural Convection Past a Vertical Plate Embedded in a Saturated Porous Medium, *Mathematical Problems in Engineering*, *2008* (2008), 689074, pp. 1-11
[17] Ogulu, A., Makinde, O. D., Unsteady Hydromagnetic Free Convection Flow of a Dissipative and Radiating Fluid Past a Vertical Plate with Constant Heat Flux, *Chemical Engineering Communications*, *196* (2009), 4, pp. 454-462
[18] Anwar, M. I., *et al*., Conjugate Effects of Heat and Mass Transfer of Nanofluids over a Non-Linear Stretching Sheet, *International Journal of Physical Sci*., *7* (2012), 26, pp. 4081-4092
[19] Khan, W. A., Pop, I., Boundary-Layer Flow of a Nanofluid Past a Stretching Sheet, *Int. J. Heat Mass Transf*., *53* (2010), 11-12, pp. 2477-2483
[20] Shakhaoath, K. M. D., *et al*., Effects of Magnetic Field on Radiative Flow of a Nanofluid Past a Stretching Sheet, *Procedia Engineering*, *56* (2013), Apr., pp. 316-322
[21] Chamka, A. J., MHD Flow of a Uniformly Stretched Vertical Permeable Surface in the Presence of Heat Generation/Absorption and a Chemical Reaction, *Int. Commun. Heat Mass Transf*., *30* (2003), Apr., pp. 413-422
[22] Afify, A., MHD Free Convective Flow and Mass Transfer over a Stretching Sheet with Chemical Reaction, *Heat Mass Transf*., *40* (2004), 6-7, pp. 495-500
[23] Gireesha, B. J., Rudraswamy, N. G., Chemical Reaction on MHD Flow and Heat Transfer of a Nanofluid Near the Stagnation Point Over a Permeable Stretching Surface with Non-Uniform Heat Source/Sink, *Int. J. Eng. Sci. Tech*., *6* (2014), Oct., pp. 13-25
[24] Olanrewaju, P. O., Makinde, O. D., Effects of Thermal Diffusion and Diffusion Thermo on Chemically Reacting MHD Boundary Layer Flow of Heat and Mass Transfer Past a Moving Vertical Plate with Suction/Injection, *Arabian Journal of Science and Engineering*, *36* (2011), 8, pp. 1607-1619
[25] Liao, S. J., *Beyond Perturbation: Introduction to the Homotopy Analysis Method*, Chapman & Hall/CRC Press, Boca Raton, Fla., USA, 2003
[26] Rashidi, M. M., Erfani, E., A New Analytical Study of MHD Stagnation-Point Flow in Porous Media with Heat Transfer, *Computers & Fluids*, *40* (2011), 1, pp. 172-178
[27] Mabood, F., *et al*., Approximate Analytical Solution for Influence of Heat Transfer on MHD Stagnation Point Flow in Porous Medium, *Computer & Fluids*, *100* (2014), Sept., pp. 72-78

Paper submitted: October 3, 2015
Paper revised: November 1, 2016
Paper accepted: November 1, 2016